The role of topological spin defects in magnetotransport of CrO_2

2007 J. Phys.: Condens. Matter 19 315206

(http://iopscience.iop.org/0953-8984/19/31/315206)

IOP PUBLISHING JOURNAL OF PHYSICS: CONDENSED MATTER

J. Phys.: Condens. Matter **19** (2007) 315206 (8pp) doi:10.1088/0953-8984/19/31/315206

The role of topological spin defects in magnetotransport of CrO_2

H Yanagihara[1] **and M B Salamon**[2]

Department of Physics and Materials Research Laboratory, University of Illinois at Urbana-Champaign, IL 61801, USA

E-mail: yanagiha@bk.tsukuba.ac.jp and salamon@uiuc.edu

Received 17 November 2006, in final form 1 February 2007
Published 3 July 2007
Online at stacks.iop.org/JPhysCM/19/315206

Abstract

We investigated the temperature dependence of the resistivity for a wide temperature range for $CrO_2(100)$ epitaxial films. The temperature derivative $d\rho/dT$ definitely shows the same character as the magnetic heat capacity anomaly in the critical regime even in a finite magnetic field and the critical exponents (α) deduced are consistent with those of 3D Heisenberg ferromagnets. In addition, we found that the spin dependent resistivity over a wide temperature range can be simply proportional to the density of diluted topological spin defects (Skyrmion strings) suggesting that those nontrivial topological defects scatter conduction electrons just like impurities. The excitation energy of such topological defects is quite comparable to that obtained by anomalous Hall effect analysis of the Ye *et al* model based on the Berry phase. The overall results give a simple picture wherein the density of the topological defects can be a dominant mechanism of resistivity, like the anomalous Hall effect. The results concerning the critical exponent analysis and intuition concerning scattering centres of magnetic disorder suggest a specific picture of the Fisher–Langer model.

(Some figures in this article are in colour only in the electronic version)

As is well known, the temperature dependent resistivity of ordinary metals is caused by electron–phonon scattering, typically leading to a T^5 temperature dependence at low temperatures. The resistivity of 'conventional' ferromagnetic metals, however, has an additive magnetic resistivity ρ_{mag} that arises from spin wave scattering and thermally excited spin disorder. Spin wave scattering is proportional to T^2 far below T_C [1, 2]; well above T_C, where the resistivity is dominated by scattering from randomly pointing spins, the magnetic resistivity is T independent because of incoherent spin disorder at such a high temperature [3, 4]. Although the spin disorder resistivity is understood quite well at very low and very high

[1] Present address: Institute of Applied Physics, University of Tsukuba, 305-8573, Japan.
[2] Present address: School of Natural Science and Mathematics, University of Texas at Dallas, USA.

temperatures, and very near T_C, there is no applicable model for explaining the behaviour for intermediate temperatures, particularly below T_C but at temperatures where the spin wave approximation is inapplicable. The situation is quite different if the ferromagnetic metal is half-metallic. Because only one spin state exists at the Fermi level, single-magnon processes are not possible; two-magnon scattering then gives a $T^{9/2}$ dependence at low temperatures, rather than a leading T^2 contribution [5]. This raises the possibility that other low energy excitations may be important in half-metallic ferromagnets.

In the last few years studies of topological (chiral) defects in 3D Heisenberg ferromagnets have led to the conclusion that, in the absence of such defects, linear spin waves are insufficient to disorder such a system [6, 7]. Subsequently, attention focused on novel aspects of the attendant spin chirality, in particular its impact on transport properties like the anomalous Hall effect (AHE) [8–12]. A Berry phase or a gauge field associated with spin chirality causes a transverse current or effective magnetic field when the conduction electrons are strongly coupled with core spins. In this paper we discuss transport data for the half-metallic ferromagnet CrO_2, taking into account the relationship between the transport properties and thermally excited topological spin defects. In particular, we show that those topological spin defects that are crucial for the AHE also contribute to ρ_{mag}.

An early consideration of the effect of chiral excitations on the AHE was in the so-called colossal magnetoresistance (CMR) manganite systems. Although the system is hole doped into the ferromagnetic metallic regime, the anomalous Hall term is electron-like while the ordinary term is hole-like. Further, the anomalous Hall coefficient R_S shows a peak above T_C. Both properties are completely dissimilar to those of conventional ferromagnetic metals such as Ni whose R_S shows a maximum just below T_C and where both R_S and R_0 have the same sign. Ye *et al* recently proposed a novel model to explain the AHE of double-exchange (DE) ferromagnetic metals such as CMR manganites in their metallic regime via topological spin defects, known as Skyrmion strings, or pairs of hedgehog–anti-hedgehog excitations [8]. In this model, nontrivial (topological) spin disorder plays an essential role in the AHE when conduction electrons are strongly coupled to core spins, as they are in DE systems. It was predicted that R_S then arises from the combination of a gauge field (associated with Skyrmion strings via the Berry phase) and spin–orbit coupling. As a result, it varies as

$$R_S \propto \frac{1}{T}\langle n\rangle \propto \frac{1}{T}\exp(-E_C/k_B T). \tag{1}$$

Here, $\langle n\rangle$ is the density of Skyrmion strings and E_C is the energy of creation of a single Skyrmion string.

For an adequate test of the Skyrmion approach, CMR systems are inappropriate; they are not pure DE ferromagnetic *metals* over a wide temperature region because, as T approaches T_C, their resistivity exceeds or is close to the Mott limit. We argue here that CrO_2 is an ideal material for exploring the effect of topological excitons. According to a recent band calculation and insight into the electronic structure given by Korotin *et al* [13], CrO_2 can be regarded as a *self-doped* DE system because of a negative charge transfer gap and the coexistence of localized and itinerant character among d electrons, strongly coupled via Hund's rule. The status of Cr ions is intermediate between those of Cr^{4+} and Cr^{3+}, like for Mn ions in the CMR manganites but with no local distortion nor any tendency for localization. For the above reasons, we have investigated AHE of CrO_2 as a pure (conventional) DE ferromagnetic material. In fact, the AHE of CrO_2 shows quantitatively good agreement with the Ye *et al* model with $E_C \approx 1100$ K (see figure 1), providing experimental evidence for the importance of topological spin defects (Skyrmion strings). The inset to figure 1 shows that the AHE is not proportional to ρ_{mag}^2 (or to ρ_{mag}) as expected conventionally for skew scattering (or side-jump) processes. Further, a scaling analysis demonstrated that $\langle n\rangle$ has the same character as the energy density in the

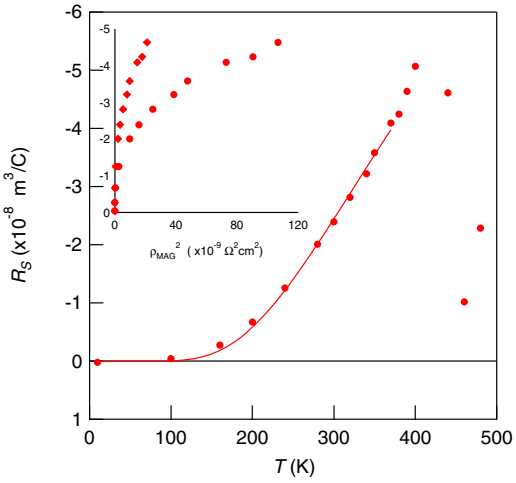

Figure 1. Temperature dependent anomalous Hall coefficient R_S of CrO_2 [12]. The solid line is a fit of equation (1). E_C of 1103 ± 28 K (∼2.9T_C) is obtained. The inset shows a test of the conventional skew scattering model for both directions.

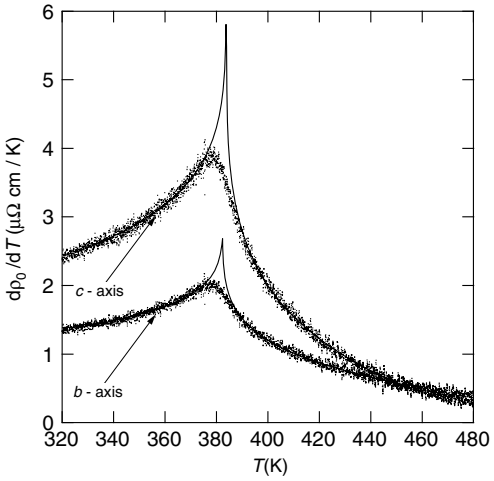

Figure 2. Temperature derivative of the resistivity $d\rho/dT$ for b and c directions. The critical exponents α obtained are -0.17 ± 0.01 for the c axis and -0.18 ± 0.02 for the b axis.

critical regime [12]. In this paper we extend the analysis to the magnetoresistance and study the relationship between ρ_{mag} and R_S.

Epitaxial CrO_2(100) films were grown by the ambient pressure chemical vapour deposition method on TiO_2(100) substrates [14]. Sample characterization, such as obtaining the crystal structure, surface flatness, and the epitaxy of the films, was carried out by x-ray diffraction and atomic force microscopy (AFM) techniques. The film was patterned into an L shape for simultaneous measurement of the resistivity in both **I** ∥ **c** and **I** ∥ **b** orientations by photolithography. Transport measurements were performed in a Quantum Design PPMS with a home-made high temperature probe over the temperature range from 5 to 480 K under a maximum magnetic field of 7 T.

The crystal structure of CrO_2 is rutile type which is basically body-centred tetragonal, so most of the physical properties show strong anisotropy. For example, the magnetization easy axis is parallel to the c direction [15]; the temperature dependence of the resistivity for **I** ∥ **c** is more distinct than that for **I** ∥ **b** [15]. This is clear in figure 2.

Within the Born approximation, the rate of scattering of conduction electrons from magnetic excitations is given by the Fisher–Langer model [16],

$$\tau^{-1}/\tau_0^{-1} = \frac{2\pi}{\sigma_0}\int_0^{\pi}\sigma(\theta)(1-\cos\theta)\sin\theta\,\mathrm{d}\theta \tag{2}$$

$$= \Gamma(0,T) + \frac{1}{8k_{\mathrm{F}}^4}\int_0^{2k_{\mathrm{F}}}\hat{\Gamma}(K,T)K^3\,\mathrm{d}K. \tag{3}$$

Here, the scattering angle is defined as θ and $\sigma(\theta)$ is the differential scattering cross section per magnetic spin. σ_0 and τ_0 are the incoherent cross section and the relaxation time well above T_{C}, respectively. $\Gamma(\mathbf{R}_i, T)$ and $\hat{\Gamma}(K, T)$ are spatial and reciprocal space spin–spin correlation functions at the given T and H, respectively. The K^3 term is a consequence of the fact that only 'large angle' scattering affects the resistance. In principle, the magnetic resistivity can be given by equation (3) and therefore $\Gamma(\mathbf{R}_i, T)$ (also $\hat{\Gamma}(K, T)$) is the essential term for the resistivity. In particular, in the critical temperature regime of ferromagnetic metals, it is known that $\hat{\Gamma}(K, T)|_{T\approx T_{\mathrm{C}}} \approx K^{\eta-2}$ with small η, meaning that large $K \approx 2k_{\mathrm{F}}$ dominates the carrier scattering process in the resistivity [16]. In other words, the resistivity anomaly is simply dominated by a short range correlation just like the energy anomaly. Therefore, the temperature derivative of the resistivity takes the same form as the heat capacity anomaly, with the same critical exponent α; that is,

$$\mathrm{d}\rho/\mathrm{d}T = (A_{\pm}/\alpha)|t|^{-\alpha} + S_0 + S_1 t, \tag{4}$$

where t is a reduced temperature $t \equiv (T - T_{\mathrm{C}})/T_{\mathrm{C}}$, $A_{\pm}$ are the coefficients at above and below T_{C}, respectively. Figure 2 shows $\mathrm{d}\rho/\mathrm{d}T$ curves for both b and c axes. Using the scaling function of equation (4), we obtain $\alpha = -0.17 \pm 0.01$ and $T_{\mathrm{C}} = 383.8 \pm 0.2$ K for the c axis data and $\alpha = -0.18 \pm 0.02$ and $T_{\mathrm{C}} = 382.4 \pm 0.3$ K for the b axis. Because of rounding from a finite size effect or lattice distortion, the temperature range of $|t| < 0.02$ is excluded from the fit. The slight discrepancy of the T_{C}s obtained in the two different directions probably comes from rounding error.

Yang *et al* recently re-investigated the magnetization and obtained the critical exponents of $\beta = 0.37$ and $\gamma = 1.43$ for CrO_2 [17]. Our α agrees quite well with the value deduced those values using the scaling relation: $\alpha = 2 - 2\beta - \gamma = -0.17$. It is also well known that the magnetic heat capacity at finite magnetic field follows the scaling law [18]

$$(C_{\mathrm{h}} - C_0)h^{\alpha/\beta\delta} = g(t/h^{1/\beta\delta}), \tag{5}$$

where h is the reduced field $M_0H/k_{\mathrm{B}}T_{\mathrm{C}}$ and C_{h} and C_0 are the heat capacity at finite and zero field, respectively. We may replace the C_{h} and C_0 by $\mathrm{d}\rho(H, T)/\mathrm{d}T$ and $\mathrm{d}\rho(0, T)/\mathrm{d}T$, if $\mathrm{d}\rho/\mathrm{d}T$ has the same character as the heat capacity anomaly in the critical regime. Figure 3 shows scaling plots of $\mathrm{d}\rho/\mathrm{d}T$ at four different fields ($\mu_0 H = 1, 3, 5, 7$ T) for both the $\mathbf{I} \parallel \mathbf{b}$ and $\mathbf{I} \parallel \mathbf{c}$ configurations. For $\mathrm{d}\rho(0, T)/\mathrm{d}T$ we used the analytical function of equation (4), fitted to the experimental data. All four data sets collapse onto a single heat-capacity-like scaling curve, as expected, suggesting that the Fisher–Langer model is valid in this DE ferromagnet. In other words, short range pair spin correlations are enough to explain the magnetoresistance in the critical regime.

Next we would like to focus on the T dependence of the resistivity over a wider temperature range. Conventional ferromagnetic metals show a T^2 dependence at low T attributed to electron–magnon scattering [1, 2]. However, because no minority spin states are available at the Fermi energy for half-metals, a single-spin-flip process cannot happen at low temperature and the single-magnon T^2 behaviour does not appear. Instead, two-magnon $T^{9/2}$ [5], T^3 [19], and $T^{3/2}$ [20] behaviours were theoretically proposed and, in fact, experimentally observed in the manganite family [21]. Most of the resistivity models that predict powers of T are applicable only in the low temperature regime ($T \lesssim 0.1T_{\mathrm{C}}$) [1] where the spin wave approximation is adequate for describing spin excitations. For CrO_2, those

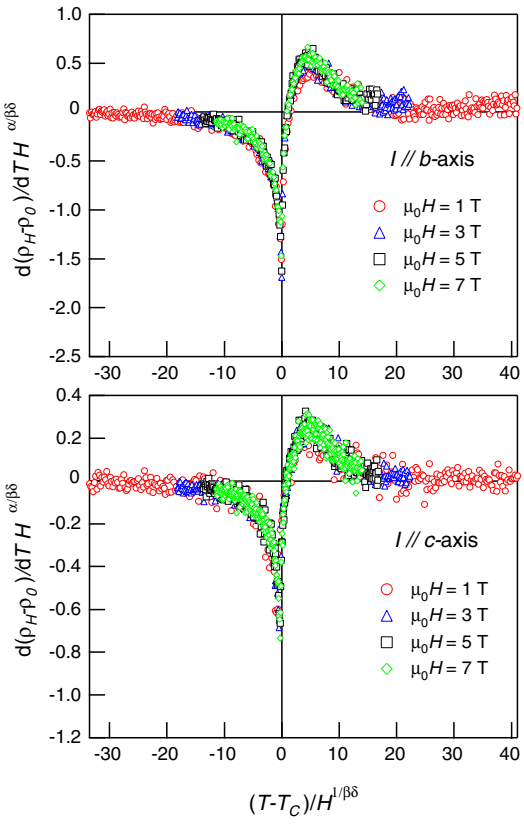

Figure 3. Scaling plot of $\mathrm{d}\rho/\mathrm{d}T$ for both b and c axes at finite fields ($\mu_0 H = 1, 3, 5, 7$ T). The critical exponents are chosen as $\alpha = -0.17$, $\beta = 0.37$ and $\delta = 1.43$.

models do not seem to hold very well [22, 23]; alternatively, there is a good phenomenological expression with a characteristic cut-off associated with the band gap of the minority spin band, $\rho(T) = \rho_0 + AT^2 \mathrm{e}^{-\Delta/k_\mathrm{B}T}$, proposed by Ranno *et al* [22–24]. However, unlike the manganites, CrO_2 presumably contains no local distortion and is supposed to be a uniform material in terms of a chemical structure. Therefore, electron–phonon scattering cannot be neglected in the resistivity analysis. Using the simplest estimation for taking account of the phonon contribution to the resistivity, we decompose the resistivity through Matthiessen's rule, considering the Bloch–Grüneisen law [25] for the lattice term,

$$\rho(T) = \rho_0 + \rho_{\mathrm{latt}}(T) + \rho_{\mathrm{mag}}(T). \tag{6}$$

Here, $\rho_{\mathrm{latt}}(T) = C_{\mathrm{BG}} \int_0^{\Theta/T} \frac{4z^5 \mathrm{d}z}{(\mathrm{e}^z - 1)(1 - \mathrm{e}^{-z})}$ and $\rho_{\mathrm{mag}}(T)$ denotes magnetic scattering term which is supposed to be T independent beyond T_C. The Debye temperature Θ is 593 K for CrO_2 [26].

As predicted by equation (2), the short range order or other small features close in size to the lattice distance should be strong contributers to $\rho_{\mathrm{mag}}(T)$. Since topological spin defects include singularities over a short distance, these will be expected to give strong magnetic scattering. Several MC simulations have revealed that the density $\langle n \rangle$ of those Skyrmion strings increases as $\mathrm{e}^{-E_\mathrm{C}/k_\mathrm{B}T}$ [6, 7, 27]. Therefore it is reasonable to assume that

$$\rho_{\mathrm{mag}}(T) = B \exp(-E_\mathrm{C}/k_\mathrm{B}T); \tag{7}$$

that is, proportional to the density of the topological spin defects with charge $Q = \pm 1$ up to the onset of critical fluctuations. A fit of the resistivity data to equation (6) is shown as solid lines in figure 4. The fit results for E_C are 1107 ± 7 K for the c axis and 1067 ± 8 K for the b axis.

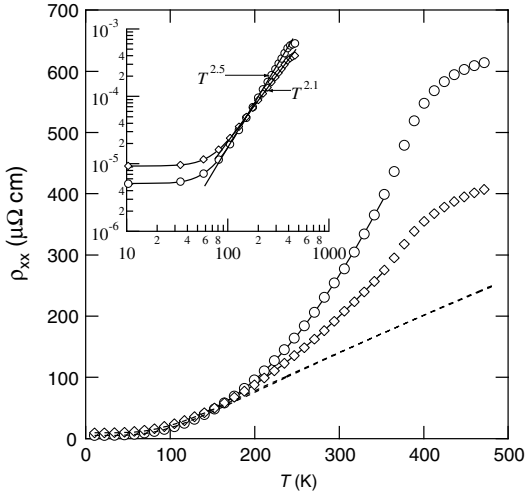

Figure 4. The raw data and fit results for the temperature dependence of the resistivity of $CrO_2(100)$ for both directions. Circles and diamonds denote $\mathbf{I} \parallel c$ axis and $\mathbf{I} \parallel b$ axis, respectively. The data are fitted by using equation (6) from the lowest temperature through 350 K. The solid lines are fit results and the dashed lines are fitted to $\rho_0 + \rho_{\text{latt}}$ for both directions and are extrapolated up to 480 K. The log–log plots are shown in the inset. The resistivity traces along the c and b axes respectively show $T^{2.5}$ and $T^{2.1}$ behaviours of which the exponents do not agree with that of the two-magnon model.

The lattice contributions are essentially the same for the two directions. This model seems to work very well from low temperature to 350 K which is close to T_C. We note that a power-law contribution, T^5 here, can be fitted to the low temperature portion of the curve. This does not fit the higher temperature contribution as shown in the inset of figure 4. The power laws that fit the data over nearly a decade in temperature are $\rho \propto T^{2.5}$ for $\mathbf{I} \parallel \mathbf{c}$ and $\rho \propto T^{2.1}$ for $\mathbf{I} \parallel \mathbf{b}$, neither of which correspond to two-magnon processes. The low temperature behaviour includes both the phonon T^5 contribution and a possible $T^{9/2}$ two-magnon term, which are indistinguishable over the narrow temperature range of the fit.

The excitation energies E_C are comparable to that obtained by AHE analysis ($E_C \approx 1100$ K $\approx 2.9T_C$) [12], but are obviously smaller than the results from the MC simulation ($E_C \sim 7T_C$) of Calderón and Brey [27]. We argue that our values are reasonable for the following reasons. In order to compare the excitation energy for any spin configurations between the Heisenberg and DE magnets, we first consider a lattice Hamiltonian for the classical Heisenberg systems, which is

$$\begin{aligned}\mathcal{H}_H &= -J_H \sum_{\langle \mathbf{x},\mathbf{y}\rangle} (\cos\theta(\mathbf{x},\mathbf{y}) - 1), \\ &\approx \tfrac{1}{2} J_H a^2 \sum_{\mathbf{x}} \sum_{\mu\alpha} (\partial_\mu S_\alpha)^2. \end{aligned} \tag{8}$$

Similarly, the simplified DE Hamiltonian can be written as

$$\begin{aligned}\mathcal{H}_{DE} &= -J_{DE} \sum_{\langle \mathbf{x},\mathbf{y}\rangle} \left(\cos\tfrac{1}{2}\theta(\mathbf{x},\mathbf{y}) - 1\right), \\ &\approx -J_{DE} \sum_{\langle \mathbf{x},\mathbf{y}\rangle} \left(\sqrt{\tfrac{1}{2}[1 + \mathbf{S}(\mathbf{x}) \cdot \mathbf{S}(\mathbf{y})]} - 1\right) \\ &\approx \tfrac{1}{8} J_{DE} a^2 \sum_{\mathbf{x}} \sum_{\mu\alpha} (\partial_\mu S_\alpha)^2 \end{aligned} \tag{9}$$

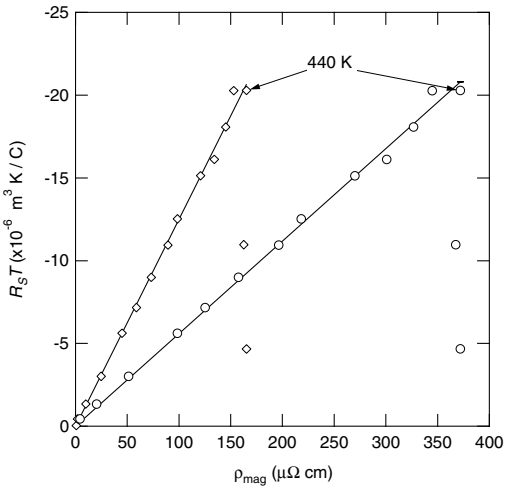

Figure 5. $R_S T$ versus ρ_{mag} plots for both directions (open circles and diamonds correspond to the ρ_{mag} for $\mathbf{I} \parallel c$ axis and of $\mathbf{I} \parallel b$ axis, respectively.) Since the ρ_{mag}s become constant at some $T^* > T_C$, the linear relation is no longer valid above $T^* \sim 440$ K.

where the summations $\sum_{\langle \mathbf{x},\mathbf{y} \rangle}$ are taken over the nearest neighbour spins and $\theta(\mathbf{x}, \mathbf{y})$ corresponds to the angle between two spins at $\mathbf{x}$ and $\mathbf{y}$ that we assume is gradually varying in a crystal. The previous MC simulation gave the value $E_C = 12.7 J_H$ [6] while Ostlund's analytical result revealed $E_C = 4\pi J_H$ for a Skyrmion string of length comparable to with lattice distance [28]. The T_C was calculated as $1.45 J_H$ [6] and therefore $E_C \approx 8.7 T_C$ for 3D classical Heisenberg magnets. For the 3D DE system, Calderón and Brey found $T_C \approx 1.06 J_{DE}$ in our notation [27]. Assuming an identical spin configuration of the topological defects to the Heisenberg model, we will obtain the E_C of πJ_{DE} by taking into account the factor four difference between equations (8) and (9). As a result, we expect $E_C \approx 3 T_C$ for 3D DE magnets. Note that the obtained $\rho_{mag}(T)$s for the different directions show strong anisotropy by a factor of 2 or so, even though the $\rho_{latt}(T)$s are almost identical. This is surprising and may imply the existence of a preferential orientation of Skyrmion strings related to the strong spin–orbit coupling.

As shown above, the origin of both the R_S and ρ_{mag} can be systematically understood through temperature dependence of the Skyrmion string density and therefore we expect $R_S T$ to be proportional to ρ_{mag} (see equations (7) and (1)). Figure 5 shows a plot of $R_S T$ and ρ_{mag} for both directions. The linear relation seems valid up to some temperature above T_C at which ρ_{mag} becomes constant due to incoherent spin disorder scattering while $R_S T$ tends to vanish. This plot suggests that the origin of AHE is similar to 'skew scattering' [29] which means that the same scattering process produces both Hall current and resistance at the same time.

To summarize, by carefully measuring magnetotransport properties such as the AHE and the resistivity of CrO_2, we have demonstrated that the temperature dependence of the magnetic resistivity of has an exponential form with the same characteristic energy as found in the AHE. This is true even though the AHE of CrO_2 is caused by the imbalance between the densities of Skyrmion strings parallel and anti-parallel to the magnetization [8] while the resistance arises from all Skyrmion strings, regardless of the magnetization orientation. That the $R_S T$ is proportional to ρ_{mag} even within the critical regime and that the critical character of $d\rho/dT$ is the same as that of the magnetic heat capacity as shown above lead us to conclude that both the AHE and magnetic resistivity arise from the density of thermally excited topological defects (Skyrmion strings). Implicit in this argument is the assumption that forward scattering, which dominates the Hall effect, occurs with an adiabatic spin rotation. The back-scattering component, which controls the resistance, does not require coherent spin rotation. Our data

appear to confirm that both the AHE and the magnetic contribution to the resistivity are controlled by the Skyrmion density to temperatures close to $0.9T_C$. The persistence of the proportionality of $R_S T$ and ρ_{mag} through the critical regime suggests that critical fluctuations have chiral character. Finally, at sufficiently high temperatures, the spin disorder becomes incoherent, losing its chiral character, leading to saturation of the magnetic resistivity and a collapse of the anomalous Hall contribution. That CrO_2 is an ideal DE, half-metallic magnet has provided an ideal system in which to demonstrate the importance of chiral spin fluctuations in determining the temperature and field dependence of transport properties.

Acknowledgments

This material is based upon work supported by the US Department of Energy, Division of Materials Sciences, under Award No. DEFG02-91ER45439, through the Frederick Seitz Materials Research Laboratory at the University of Illinois at Urbana-Champaign.

References

[1] Volkenshtein N V, Dyakina Y P and Startsev V E 1973 *Phys. Status Solidi* b **57** 9
[2] Campbell I A and Fert A 1982 *Transport Properties of Ferromagnets in Ferromagnetic Materials* vol 3, ed E P Wohlfarth (Amsterdam: North-Holland) chapter 9, p 747
[3] Kasuya T 1956 *Prog. Theor. Phys.* **16** 58
[4] de Gennes P and Friedel J 1958 *J. Phys. Chem. Solids* **4** 71
[5] Kubo K and Ohata N 1972 *J. Phys. Soc. Japan* **33** 21
[6] hot Lau M and Dasgupta C 1989 *Phys. Rev.* B **39** 7212
[7] Holm C and Janke W 1994 *J. Phys. A: Math. Gen.* **27** 2553
[8] Ye J, Kim Y B, Millis A J, Shraiman B I, Majumdar P and Tešanović Z 1999 *Phys. Rev. Lett.* **83** 3737
[9] Chun S H, Salamon M B, Lyanda-Geller Y, Goldbart P M and Han P 2000 *Phys. Rev. Lett.* **84** 757
[10] Taguchi Y, Oohata Y, Yoshizawa H, Nagaosa N and Tokura Y 2001 *Science* **291** 2573
[11] Lyanda-Geller Y, Chun S H, Salamon M B, Goldbart P M, Han P, Tomioka Y and Tokura Y 2001 *Phys. Rev.* B **63** 184426
[12] Yanagihara H and Salamon M B 2002 *Phys. Rev. Lett.* **89** 187201
[13] Korotin M A, Anisimov V I, Khomskii D I and Sawatzky G A 1998 *Phys. Rev. Lett.* **80** 4305
[14] Ishibashi S, Namikawa T and Satou M 1979 *Mater. Res. Bull.* **14** 51
[15] Li X W, Gupta A, McGuire T R, Duncombe P R and Xiao G 1999 *J. Appl. Phys.* **85** 5585
[16] Fisher M E and Langer J S 1968 *Phys. Rev. Lett.* **20** 665
[17] Yang F Y, Chien C L, Li X W, Xiao G and Gupta A 2001 *Phys. Rev.* B **63** 092403
[18] Ho J T 1971 *Phys. Rev. Lett.* **26** 1485
[19] Furukawa N 2000 *J. Phys. Soc. Japan* **69** 1954
[20] Wang X and Zhang X-G 1999 *Phys. Rev. Lett.* **82** 4276
[21] Akimoto T, Moritomo Y, Nakamura A and Furukawa N 2000 *Phys. Rev. Lett.* **85** 3914
[22] Watts S M, Wirth S, von Molnár S, Barry A and Coey J M D 2000 *Phys. Rev.* B **61** 9621
[23] Liu S J, Juang J Y, Wu K H, Uen T M, Gou Y S and Lin J Y 2002 *Appl. Phys. Lett.* **80** 4202
[24] Ranno L, Barry A and Coey J M D 1997 *J. Appl. Phys.* **81** 5774
[25] Ziman J M 1972 *Principles of the Theory of Solids* 2nd edn (Cambridge: Cambridge University Press) chapter 7
[26] Barry A, Coey J M D, Rannno L and Ounadjela K 1998 *J. Appl. Phys.* **83** 7166
[27] Calderón M J and Brey L 2001 *Phys. Rev.* B **63** 054421
[28] Ostlund S 1981 *Phys. Rev.* B **24** 485
[29] Hurd C M 1972 *The Hall Effect in Metals and Alloys* (New York: Plenum Press)